Prediction of rainfall runoff-induced sediment load from bare land surfaces by generalized regression neural network and empirical model

Gokmen Tayfur [ID] [1], Hafzullah Aksoy[2] & Ebru Eris[3]

[1]Department of Civil Engineering, Izmir Institute of Technology, Izmir, Turkey; [2]Department of Civil Engineering, Istanbul Technical University, Istanbul, Turkey; and [3]Department of Civil Engineering, Ege University, Izmir, Turkey

Abstract

Based on three rainfall run-off-induced sediment transport data for bare surface experimental plots, the generalized regression neural network (GRNN) and empirical models were developed to predict sediment load. Rainfall intensity, slope, rainfall duration, soil particle median diameter, clay content of the soil, rill density and soil particle mass density constituted the input variables of the models while sediment load was the target output. The GRNN model was trained and tested. The GRNN model was found successful in predicting sediment load. Sensitivity analysis by the GRNN model revealed that slope and rainfall duration were the most sensitive parameters. In addition to the GRNN model, two empirical models were proposed: (1) in the first empirical model, all the input variables were related to the sediment load, and (2) in the second empirical model, only rainfall intensity, slope and rainfall duration were related to the sediment load. The empirical models were calibrated and validated. At the calibration stage, the coefficients and the exponents of the empirical models were obtained using the genetic algorithm optimization method. The validated empirical models were also applied to two more experimental data sets: (1) one data set was from a field experiment, and (2) one set was from a laboratory experiment. The results indicated the success of the empirical models in predicting sediment load from bare land surfaces.

Introduction

Catchment sediment yield is a direct indication of surface erosion induced by rainfall run-off. Surface erosion by rainfall and run-off embodies the processes of detachment, transportation and deposition of soil particles (Foster, 1982). Detachment occurs when the erosive forces of raindrop impact (and/or flowing water) exceed the resistance of soil to the erosion. Detached particles are then carried downstream by surface run-off. Deposition occurs when sediment load exceeds the transport capacity of flow (Romkens et al., 2002).

Surface erosion by rainfall and run-off is also the primary source of fine sediment being transported to the receiving water bodies. As such, erosion can not only reduce the productivity of croplands but also degrade the water quality because of the association of pollutants to the fine sediment particles (Nord and Esteves, 2005; Julien, 2010). The deposition of the transported sediment in water conveyance structures such as irrigation canals, stream channels, reservoirs, estuaries and harbours can limit the functions of these structures (Aksoy and Kavvas, 2005). Underestimation of the dead storage volume of a dam reservoir can shorten the project life of the reservoir. Overestimation of the dead storage, on the other hand, can result in unnecessary cost. River navigation and restoration projects, like dam reservoir planning, require the estimates of sediment loads from upland areas and transported within rivers. Hence, the rainfall run-off-induced erosion and sediment transport have been the topic of research for many decades.

Rainfall run-off-induced erosion on land surfaces has been experimentally studied by many researchers using laboratory flumes and/or experimental plots in the field (Wischmeier et al., 1971; Kilinc and Richardson, 1973; Meyer et al., 1975; Barfield et al., 1983; Govindaraju et al., 1992; Abrahams et al., 1998; Portner and Schleiss, 2001; Nunes et al., 2006; de Lima et al., 2011, Aksoy et al., 2012; Montenegro et al., 2013). Modelling studies, at the same time, have been carried out for the erosion and sediment transport processes. Approaches ranged

from simple conceptualization to the process-based modelling (Govindaraju and Kavvas, 1991; 1992; Tayfur, 2001; 2002a; Merritt *et al.*, 2003; Aksoy and Kavvas, 2005; Julien, 2010).

Conceptual models require relatively less information than the process-based models, which often require numerical methods for the solution of governing equations (Storm *et al.*, 1987; Govindaraju and Kavvas, 1991; 1992; Tayfur and Singh, 2004; Tayfur, 2007; Julien, 2010). They can provide gross estimates of the sediment load at the outlet of land surfaces while the distributed process-based models can also produce temporal and spatial variation of the variables over the surface. The process-based models are effective provided that the spatial and temporal distribution of the required data is available and the objective is to develop local mitigation measures to prevent erosion, and sediment and contaminant transport (Tayfur and Singh, 2004).

One of the major shortcomings of the existing empirical (conceptual) models is their limited applicability. In other words, they are effective only when the laboratory (or field) experiments from which they are derived are satisfied (Aksoy and Kavvas, 2005). These models mostly relate sediment rate to one or higher number of variables such as run-off rate, bed slope, rainfall intensity and sediment particle diameter (Meyer and Wischmeier, 1969; Kilinc and Richardson, 1973; Foster, 1982; Julien and Simons, 1985; Gilley *et al.*, 1992; Zhang *et al.*, 2009; Grismer, 2011; Aksoy *et al.*, 2013; 2017). They require the measurements of the flow rates from land surfaces to be able to make good estimates of sediment loads. This is another shortcoming of the empirical models, especially for the ungauged basins. Furthermore, the existing empirical models do not consider rainfall duration as an input variable, implicitly assuming that rainfall duration has no effect on soil loss. However, experiments have shown that as the rainfall duration increases, sediment rate increases (Kilinc and Richardson, 1973, Katebikord *et al.*, 2017). Approaching the problem by means of a different methodology, Tayfur (2002b) employed the Feed Forward Neural Network (FFNN) to predict sediment load on the data of Kilinc and Richardson (1973) by considering the slope and rainfall intensity as input variables.

The objective of this study is twofold: (1) to apply the Generalized Regression Neural Network (GRNN) to predict sediment load from bare slopes, and (2) to develop more comprehensive empirical models, which would have a wide range of applicability, for the same predictive purpose. The development of the models was carried out by considering in the input vector, data sets within a wide range of slope, rainfall duration, rainfall intensity, sediment particle density and diameter, rill density and the clay content of the soil. This is the first study considering rainfall duration, sediment particle density, rill density and the clay content of the soil along with other major variables to predict sediment load from bare slopes. Also, this study is the first to apply the GRNN in the rainfall run-off sediment transport modelling literature. The GRNN was preferred as it has basically two major advantages over the FFNN: that it does not face local minima problem, and it does not generate physically implausible values (Cigizoglu, 2005).

Data collection

Three data sets were obtained from the literature. The first data set was obtained from Kilinc and Richardson (1973) who carried out rainfall run-off-induced erosion and sediment transport experimental runs over a flume, 1.5 m-wide, 4.9 m-long, and with an adjustable bed slope. The soil was sand with 10% clay content and there was no rill over the surface of the experimental plot. The mean sediment particle diameter was 0.35 mm and the soil density 2634 kg/m^3. The experiments were carried out over six bare surfaces with bed slopes of 5.7, 10, 15, 20, 30 and 40% subjected to four rainfall intensities of 32, 57, 93 and 117 mm/h. Sediment load was measured at different intervals of rainfall duration which lasted 60 minutes at most. From Kilinc and Richardson (1973), a total of 193 sets of sediment load measured at different rainfall durations, under different rainfall intensities, and over different bed slopes were compiled.

The second set of data was obtained from Aksoy *et al.* (2011)) who carried out rainfall run-off-induced erosion and sediment transport experiments over a 1.4 m-wide and 6.5 m-long flume having an adjustable slope within the range of 5–20%, both at the longitudinal and the lateral directions. Four different rainfall intensities (45, 65, 85, 105 mm/h) were applied. Two different size sands were used as sediments: (1) sand with a mean diameter of 0.45 mm and a density of 2650 kg/m^3 and (2) sand with a mean diameter of 0.15 mm and a density of 2600 kg/m^3. Before the rain is applied in each experiment, a rill was pre-formed on the plot having a 26 cm width, amounting to 19% rill density. In total, 80 sets of experiments, with 15-minute rainfall duration, were carried out.

The third data set was obtained from Katebikord *et al.* (2017) who carried out experiments over a 1 m^2 field experimental plot under 40 mm/h rainfall intensity and 18% slope. The soil texture was loam-clay having 0.023 mm particle diameter and 2786 kg/m^3 density. A total of 18 runs were carried for 6 different rainfall durations, ranging from 5 to 30 minutes.

Generalized regression neural network (GRNN)

The GRNN, which does not have a local minima problem and does not make physically implausible predictions, was employed in this study. It is a method for estimating a joint probability density function (pdf) of x and y given only a training set. If $f(x,y)$ represents the joint continuous pdf of the vector random variable x and the scalar random variable y, the estimation can be expressed as:

$$E\left[y \mid x\right] = \frac{\int\limits_{-\infty}^{\infty} y f(x,y)\,dy}{\int\limits_{-\infty}^{\infty} f(x,y)\,dy} \tag{1}$$

The pdf $f(x,y)$ is usually estimated from a sample of the observations of the variables, x and y (Cigizoglu, 2005):

$$\hat{f}(x,y) = \frac{1}{(2\pi)^{(p+1)/2}\,\sigma^{(p+1)}}\frac{1}{n}\sum_{i=1}^{n}\exp\left[-\frac{(x-x_i)^T(x-x_i)}{2\sigma^2}\right]\exp\left[-\frac{(y-y_i)^2}{2\sigma^2}\right] \tag{2}$$

where $\hat{f}(x,y)$ is the probability estimator, which is based on the sample values x_i and y_i of the random variables x and y, respectively; n is the number observation in the sample, σ is the smoothing parameter and p is the dimension of the vector variable x.

A physical interpretation of the probability estimate $\hat{f}(x,y)$ is that it assigns the sample probability of width σ for each sample x_i and y_i, and the probability estimate is the sum of the sample probabilities. Let us define the scalar function d_i as:

$$d_i^2 = (x-x_i)^T(x-x_i) \tag{3}$$

and substitute it into Eq. (2). Performing the indicated summations in Eq. (2) yields the estimation of output variable, y as:

$$\hat{y}(x) = \frac{\sum\limits_{i=1}^{n} y_i \exp\left(-\frac{d_i^2}{2\sigma^2}\right)}{\sum\limits_{i=1}^{n} \exp\left(-\frac{d_i^2}{2\sigma^2}\right)} \tag{4}$$

When σ is made large, the estimated density is forced to be smooth and at the limit, it becomes a multivariate Gaussian function with the covariance σ^2 (Cigizoglu, 2005). On the other hand, a smaller value of σ allows the estimated density to assume non-Gaussian shapes, but with a disadvantage that extreme points may have a negative effect on the estimate. Its optimal value is often determined experimentally (Kim *et al.*, 2013). Eq. (4) is directly applicable to problems involving numerical data. The only parameter which should be adjusted in the GRNN simulations is the smoothing parameter, σ (Cigizoglu, 2005).

The GRNN structure has four layers (Fig. 1): input, pattern, summation and output (Tsoukalas and Uhrig, 1997). Neurons in each layer are fully connected to each other. In this study, the number of input units in the first layer is equal to the total number of input variables, which are the rainfall intensity (R), slope (S), rainfall duration (T_d), particle median diameter (D_{50}), clay content (λ_c), rill density (λ_r) and particle mass density (ρ_s). The second layer has the pattern units; its outputs are passed on to the summation units in the third layer. Each unit in the pattern layer represents a training pattern and its output is a measure of the distance of the input from the stored patterns. The summation layer has two units, the S-summation neuron and the D-summation neuron (Seckin *et al.*, 2013). The S-summation neuron computes
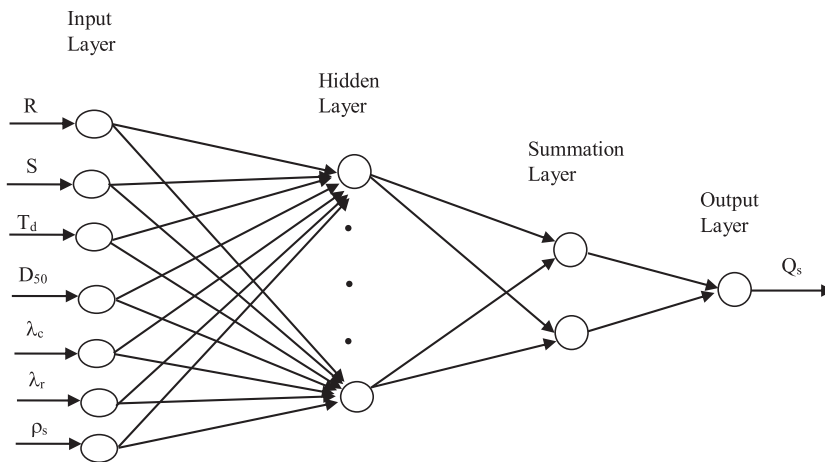

Fig. 1. Schematic representation of the GRNN model.

the sum of the weighted outputs of the pattern layer while the D-summation neuron does the same for the non-weighted outputs. The connection weights are set unity between the pattern layer neurons and the D-summation neuron (Kim *et al.*, 2013).

The output layer divides the output of each S-summation neuron by that of each D-summation neuron, yielding the predicted value to an unknown vector, which is the sediment load (Q_s) in this study. This can be, following Eq. (4), expressed as:

$$\hat{Q}_s(x) = \frac{\sum_{i=1}^{n} Q_{si} \exp\left(-\frac{d_i^2}{2\sigma^2}\right)}{\sum_{i=1}^{n} \exp\left(-\frac{d_i^2}{2\sigma^2}\right)} \qquad (5)$$

It should be noted that the GRNN is not a conceptual or an empirical model. It is one type of the artificial neural network (ANN) algorithms. The majority of the ANN applications in hydrology have involved the employment of the back propagation training algorithm in the FFNN (Tayfur, 2012). However, the FFNN algorithm has two major drawbacks: (1) they are very sensitive to the selected initial weight values, thus they can provide results differing from each other significantly, and (2) the local minima issue is a major problem. During the training stage, the network can be sometimes trapped by the local error minima preventing them to reach the global minimum. On the other hand, the GRNN does not require an iterative training procedure as in the back propagation method.

It approximates any arbitrary function between the input and output vectors, drawing the function estimate directly from the training data. As stated above, the GRNN simulations do not face the frequently encountered local minima problem in the FFBP applications and the GRNN does not generate estimates that are not physically plausible (Cigizoglu and Alp, 2006).

Further details of the GRNN can be found elsewhere (Tsoukalas and Uhrig, 1997; Cigizoglu and Alp, 2006; Alp and Cigizoğlu, 2007; Tayfur, 2012; Seckin *et al.*, 2013; Kim *et al.*, 2013). In this study, NeuroTools, the package program of Palisade Corporation (2012), was used.

GRNN application

The input vector for the GRNN was formed using the rainfall intensity (R), slope (S), rainfall duration (T_d), particle median diameter (D_{50}), clay content of the soil (λ_c), rill density (λ_r) and soil mass density (ρ_s). The sediment rate (Q_s) is the target output. A total of 233 data sets were used, of which 163 (70%) for the training (calibration) of the network and the rest (30%) for the testing (validation). The units of the variables in the training and testing were as follows: clay content (%), rill density (%), particle mass density (kg/m³), particle diameter (mm), rainfall intensity (mm/h), slope (%), rainfall duration (min) and sediment discharge (kg/m²).

Figure 2 presents the measured versus predicted total sediment loads for the training and testing stages of the constructed GRNN model. As seen in Fig. 2, the GRNN
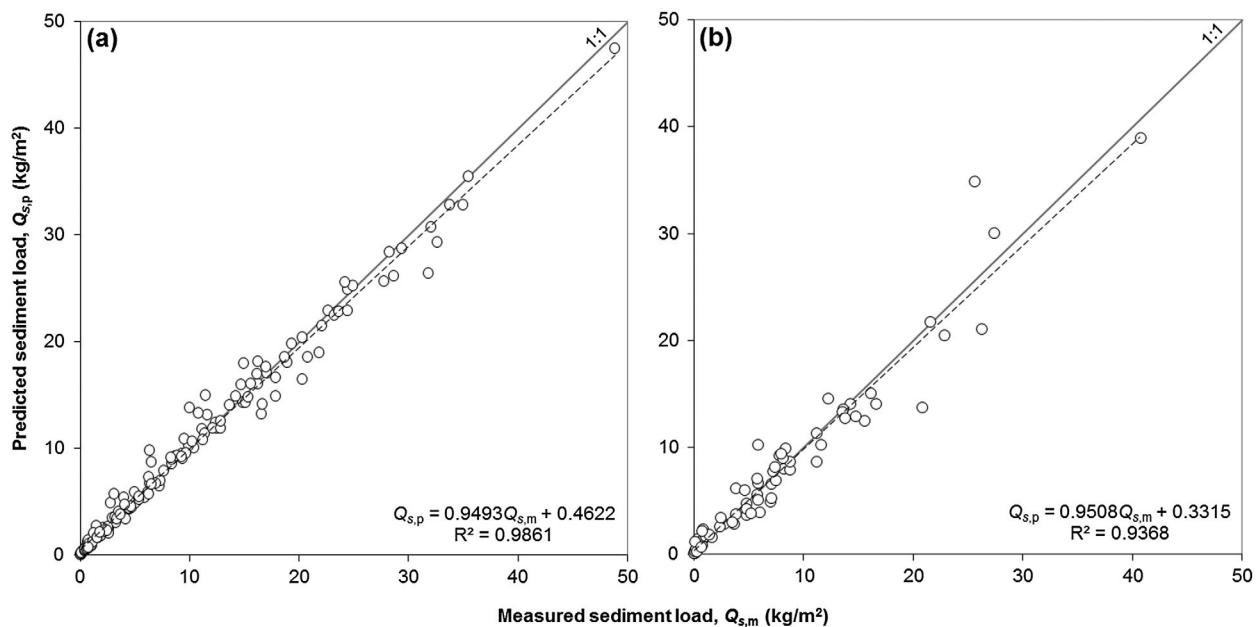

Fig. 2. Sediment load, measured versus predicted by the GRNN model; (a) Training stage, (b) Testing stage.

was successfully trained with the root mean squared error (RMSE) of 1.182 kg/m². The coefficient and the intercept of the fitted linear equation were found close to one and zero, respectively. The distribution of the data around the perfect-fit (1 : 1) line is even, the determination coefficient (R^2) is 0.9861, implying a successful training (Sen, 2004; Tayfur, 2012). As explained previously, the only parameter which should be adjusted in the GRNN simulation is the smoothing parameter, σ. The lowest RMSE and the highest R^2 values for the training period were obtained with $\sigma = 0.12$.

Figure 2 also shows that the model can confidently be used for the prediction purpose. It predicted with RMSE = 2.009 kg/m² and $R^2 = 0.9368$. As it was in the training stage, the distribution of the data around the perfect-fit line is even, successfully predicting all values, including the low and high sediment loads. The coefficient and the intercept of the fitting line are close enough to one and zero, respectively.

Sensitivity analysis by GRNN

A sensitivity analysis is carried out to see the most sensitive parameters. For this purpose, in the input vector of the GRNN model, in each case, one variable was not considered. For example, in the first case, all the variables except D_{50} were considered in the input vector. Similarly, in the second case, all the variables but particle density were taken as the input parameters. As seen in Table 1, the most sensitive parameters were found to be the slope and the rainfall duration. Other parameters have a comparable sensitivity, not as significant as the slope and the rainfall duration.

Empirical models

Empirical models in the forms of

$$Q_s = \alpha_1 \left(1 - \lambda_c\right)^{\beta 1} \left(1 + \lambda_r\right)^{\beta 2} \rho_s^{\beta 3} R^{\beta 4} S^{\beta 5} T_d^{\beta 6} D_{50}^{\beta 7} \qquad (6)$$

$$Q_s = \alpha_2 R^{\eta 1} S^{\eta 2} T_d^{\eta 3} \qquad (7)$$

were proposed in this study. In Eqs (6) and (7) α_1 and α_2 are the coefficients, β_1, β_2, β_3, β_4, β_5, β_6, β_7, η_1, η_2, and η_3 are the exponents, whose optimal values are obtained by the genetic algorithm (GA). The clay content of the soil texture would reduce the erosion. Therefore, in Eq. (6), it was subtracted from the unity; i.e.; the soil becomes 100% sand when the clay content is zero. On the other hand, rill flow would increase erosion and sediment transport since its transport capacity is higher than

Table 1 Sensitivity analysis of the variables; rainfall intensity (R), slope (S), rainfall duration (T_d), particle median diameter (D_{50}), clay content (λ_c), rill density (λ_r) and soil particle mass density (ρ_s)

Case	Input vector	Unused variable in the input vector of GRNN	RMSE (kg/m²)	R^2
Case 1	$R, S, T_d, \lambda_c, \lambda_r, \rho_s$	D_{50}	3.87	0.88
Case 2	$R, S, T_d, D_{50}, \lambda_c, \lambda_r$	ρ_s	2.90	0.91
Case 3	$R, S, T_d, D_{50}, \lambda_r, \rho_s$	λ_c	3.30	0.89
Case 4	$R, S, T_d, D_{50}, \lambda_c, \rho_s$	λ_r	3.14	0.90
Case 5	$R, T_d, D_{50}, \lambda_c, \lambda_r, \rho_s$	S	6.29	0.48
Case 6	$R, S, D_{50}, \lambda_c, \lambda_r, \rho_s$	T_d	5.40	0.70

that over the interrill areas (Govindaraju and Kavvas, 1992; Tayfur, 2007). That is why the rill density was added to the unity in Eq. (6). Equation (7) was proposed based upon the results of the sensitivity analysis obtained by the GRNN. The GA optimization method was employed as explained below to obtain the optimal values of the exponents and the coefficients of the proposed empirical models.

Genetic algorithm (GA) and its implementation

The genetic algorithm (GA) which has recently found wide applications in water resources engineering (Sen and Oztopal, 2001; Jain *et al.*, 2004; Guan and Aral, 2005; Singh and Datta, 2006; Tayfur and Moramarco, 2008; Tayfur, 2009; Tayfur *et al.*, 2009; Tayfur and Singh, 2011; Aksoy *et al.*, 2016, 2017; Tayfur, 2017) is a nonlinear search and optimization method inspired by the biological processes of the natural selection and the survival of the fittest. It makes relatively few assumptions and does not rely on any mathematical properties of the functions such as the differentiability and the continuity. This makes it generally applicable and robust (Liong *et al.*, 1995; Goldberg, 1989). The basic units of the GA consist of '*bit*', '*gene*', '*chromosome*' and '*gene pool*'. A *gene* consisting of bits [0 and 1] represents a model parameter (or a decision variable) to be optimized. The combination of the genes forms the *chromosome,* each of which is a possible solution for each variable. Finally, a set of chromosomes forms the *gene pool.* The main GA operations basically consist of the *generation of initial gene pool, evaluation of fitness for each chromosome, selection, cross-over* and *mutation.* Details of the GA can be obtained from Goldberg (1989) and Tayfur (2012), among others.

The GA can minimize (or maximize) an objective function under given constraints. In this study, the GA was employed to obtain the optimal values of the exponents and coefficients of the empirical models by minimizing the mean absolute error (MAE) between the measured sediment load and that calculated by the model.

The data sets randomly separated for the training and testing of the GRNN model were herein used, respectively, for the calibration and validation of the GA-based empirical models. Hence, 163 sets of the same data as in the GRNN model were employed to find the optimal values of the coefficients and the exponents of the empirical models (Eqs (6) and (7) by minimizing the MAE. For this purpose, 120 chromosomes, 80% crossover, 4% mutation rate and 16 000 iterations were used in Evolver, the GA package software of Palisade Corporation (2012). The calibrated (optimal) values of the coefficients are summarized in Table 2. The exponents of the particle density (ρ_s) and the particle diameter (D_{50}) are negative, implying that sediment rate inversely varies with these variables. Similarly, the exponent of the slope is between 1 and 2, agreeing with the literature (Aksoy and Kavvas, 2005; Aksoy *et al.*, 2017). Figure 3 compares the measured

sediment load versus that predicted by Eq. (6) for the calibration stage. As seen, the coefficient and the intercept of the best-fit line are close to one and zero, respectively, RMSE is 2.68 kg/m² and R^2 is 0.9226, all implying a successful calibration. The same 70 data sets used for testing the GRNN model were predicted to check the validity of the model (Eq. (6) by using the optimal values of the parameters in Table 2. The performance of the model for the validation stage is also shown in Fig. 3. It is seen that the RMSE is 2.33 kg/m² and R^2 is 0.9156. The distribution of the data around the perfect-fit line is almost even; the model successfully predicts low and high values.

Equation (7) relates the sediment rate to the rainfall, slope and rainfall duration, as discussed above. The same 163 data sets used for the training of the GRNN and the calibration of Eq. (6) were employed herein to obtain the optimal values of the coefficient and the exponents of Eq. (7) by using the GA optimization model. Figure 4 shows the measured versus predicted sediment loads, as a result of the performed calibration. Although the data are evenly distributed along the best-fit line, high values are underestimated in general. At the calibration stage,

Table 2 Optimal values of the coefficients and the exponents of the empirical models

	α_1	β_1	β_2	β_3	β_4	β_5	β_6	β_7
Empirical model 1 (Eq. (6))	0.1647	4.0714	5.8937	−1.3561	1.7114	1.2104	0.9776	−0.1855
	α_2	η_1	η_2	η_3				
Empirical model 2 (Eq. (7))	0.00045	1.2952	0.7419	0.5680				
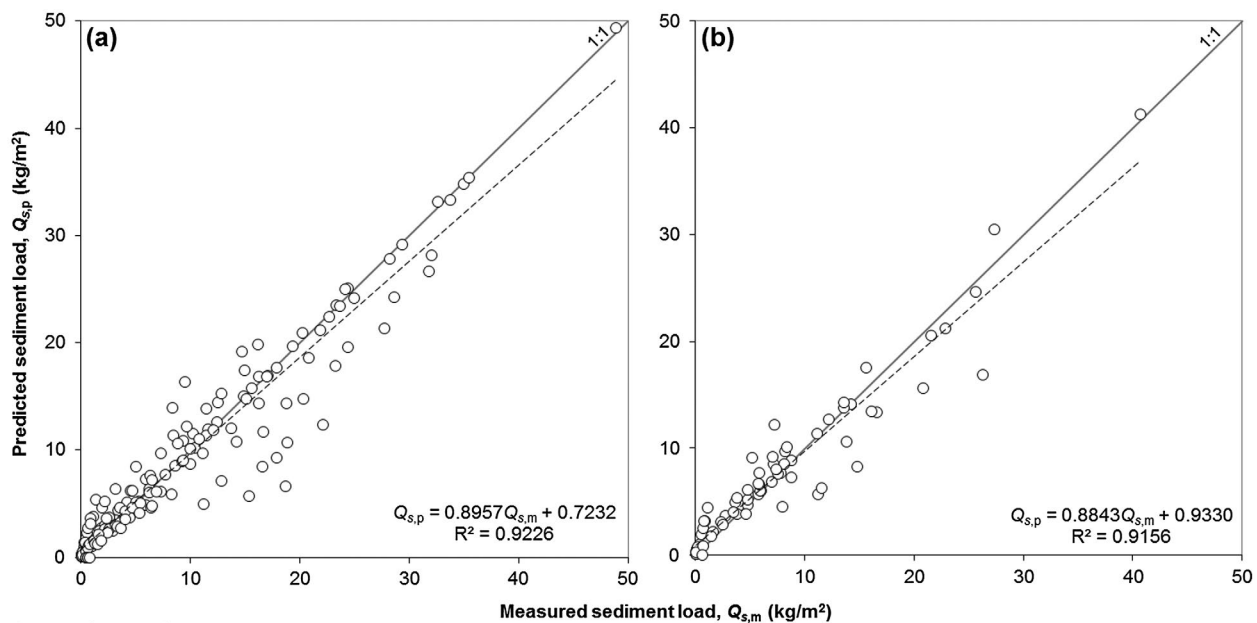
Fig. 3. Sediment load, measured versus predicted by the empirical model – Eq. (6) – (a) Calibration stage, (b) Validation stage.
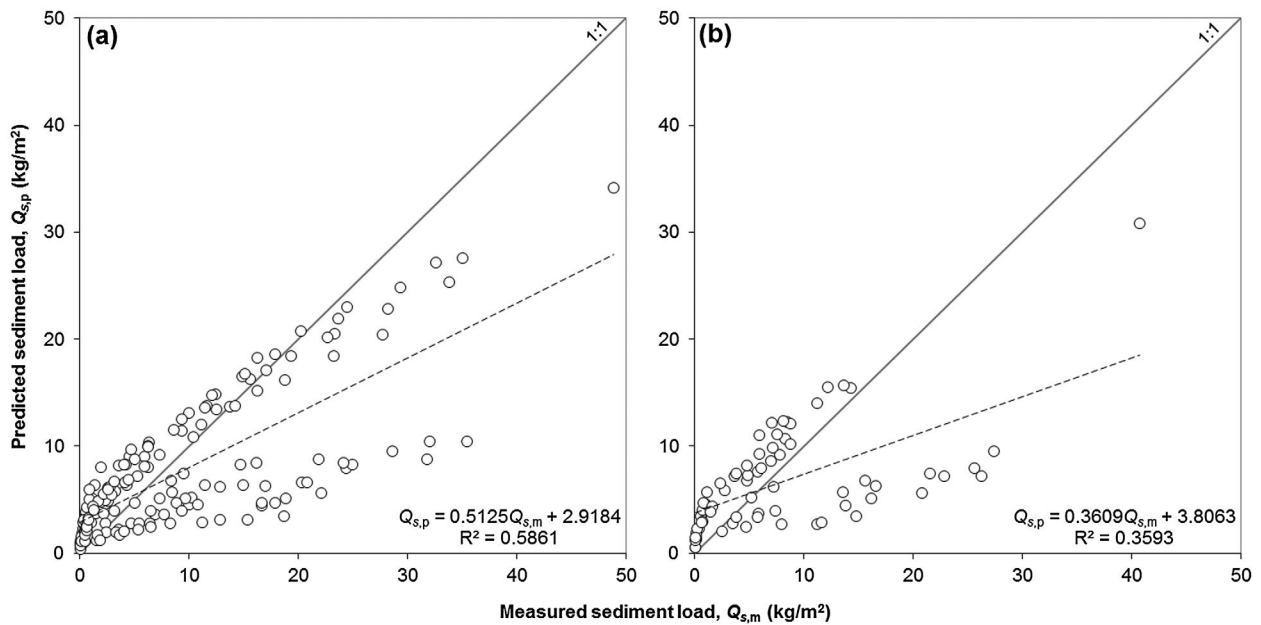
Fig. 4. Sediment load, measured versus predicted by the empirical model – Eq. (7) – (a) Calibration stage, (b) Validation stage.

RMSE = 6.41 kg/m^2 (higher than the previous cases) and R^2 = 0.58 (lower than the previous cases). The optimal values of the coefficient and the exponents in the best-fit line are given in Table 2. The application of Eq. (7), with the so-obtained optimal values for the data in the validation stage, resulted in a high RMSE of 6.50 kg/m^2 and a low R^2 of 0.36. Figure 4 also shows the results of the validation stage for Eq. (7). A clear underestimation problem is seen although the distribution of the data is even. The results indicate that when the data especially come from a rilled surface or clay soils, empirical models in the form of Eq. (7) may not be sufficient enough for the purpose of sediment load prediction.

As it was the case in the GRNN model, it should be noted that the units of the variables in Eqs (6) and (7) are as follows: clay content (%), rill density (%), particle mass density (kg/m^3), particle diameter (mm), rainfall intensity (mm/h), slope (%), rainfall duration (min) and sediment discharge (kg/m^2). If one were to work with different units, the model calibration should be redone accordingly.

Application to field experimental data

Equations (6) and (7) were applied to estimate the total sediment load from the field experiment carried out in September 1992 (Govindaraju *et al.*, 1992) over a hill slope in Buckhorn Summit, California, USA. A steep hill slope section with 66.7% slope, 10 m width and 15 m length was subjected to 152.4 mm/h rainfall for a 12-minute

duration (Govindaraju *et al.*, 1992). The decomposed granite soil had size particles of, on the average, D_{50} = 0.625 mm (Govindaraju *et al.*, 1992). The soil mass density was about 2580 kg/m^3 and the rill density over the experimental section was observed to be almost 32% (Govindaraju *et al.*, 1992). The total sediment load was measured as 199.2 kg/m^2. With the given inputs, Q_s was calculated as 217.4 kg/m^2 by Eq. (6) with a relative error of 9.1%. If one were to apply Eq. (7) with the given inputs, Q_s was obtained as 28 kg/m^2, which is sevenfold less than the measured sediment load. Eq. (7) significantly underestimated the sediment load. Its poor performance is connected mainly to the fact that it does not consider the particle diameter, particle density, clay content and the rill density among which the rill density has a particular importance as Govindaraju *et al.* (1992) observed from the experiments that most of the sediment came down from the rill sections.

The empirical models (Eqs (6) and (7) were also applied on a data set from an experimental flume of 9% slope, subjected to 100 mm/h rainfall for a duration of 30 minutes with yellow podzolic soil of 0.2 mm-diameter and 1480 kg/m^3 mass density (Singer and Walker, 1983). No rilling was taken into account in the experiments. The total sediment load measured in the experiments was 12.8 kg/m^2. The predictions of Eqs (6) and (7) were 11.7 kg/m^2 with 8.6% error and 6.15 kg/m^2 with 52% error, respectively. Although the error is quite high, Eq. (7) could be considered for a gross prediction of total sediment load from a surface with no rill.

Discussion

A total of 233 data sets belonging to different experimental studies were compiled from the literature to develop the GRNN and the empirical models for the prediction of rainfall run-off-induced sediment load from bare and rilled land surfaces. The data covered a wide range of rainfall duration (5–60 minutes), rainfall intensity (32–117 mm/h), bed slope (5.7–40%) and particle size (0.023–0.45 mm median diameter). The clay content of the soil, rill density, particle mass density, particle diameter, rainfall intensity, slope, rainfall duration and sediment discharge were used in the development of the models.

From the data sets, 163 items were used in training the GRNN and 70 for testing it. It is the first time that the GRNN was applied to predict the rainfall run-off-induced sediment load from bare and rilled surfaces. The model did not produce any physically plausible negative values. It converged fast and did not get trapped in a local minimum. This implies that when the necessary input data are available, the GRNN can be confidently used to make predictions, even for ungauged basins.

As far as the empirical models are concerned, the first model (Eq. (6) expresses the sediment load as a function of the same input variables used in the GRNN model while the second model (Eq. (7) expresses the sediment load as a function of only the slope, rainfall intensity and rainfall duration. The coefficients and the exponent of the empirical models were optimized by the GA using the same 163 data items employed in the training of the GRNN. The calibrated empirical models were then validated with the rest of the data (70 items used for the testing of the GRNN). The empirical equations were further validated against different laboratory and field data from the literature. The results indicate that Eq. (6) can be employed to predict loads from bare rilled surfaces. It has a general applicability and therefore it can be used for ungauged sites. Eq. (7), on the other hand, has a limited range of applicability such that it cannot yield reliable results when the bare surfaces contain rills and high content of clay. The results indicate that the rill density and rainfall duration play as important roles as the slope. Therefore, these parameters should not be ignored in the rainfall run-off-induced sediment transport studies.

When the applicability of the empirical models (Eq. (6) particularly) is concerned, the availability of the input variables becomes an issue. The input variables seem quite specific. However, fast development in mapping with incorporation of space technology such as remote sensing and satellites is considered helpful to derive a fine-tuned topography to get the slope and the rilling structure

(Shaker *et al.*, 2010; Desprats *et al.*, 2013; Fiorucci *et al.*, 2015). In this regard, support by the Geographical Information Systems (Yuksel *et al.*, 2008; Animka *et al.*, 2013; Ganasri and Ramesh, 2016; Gelagay and Minale, 2016) is unavoidably necessary. Other inputs in the empirical model are meteorology related which are generally available at some near points. The proposed models (the GRNN and the empirical models) can be used to predict sediment load from ungauged sites provided that the input variables are made available by the use of up-to-date technologies.

Conclusions

The following conclusions are drawn from this study:

(1) The GRNN can be a useful tool for the prediction of sediment load from bare and rilled land surfaces. The input vector of the GRNN model is composed of rainfall intensity, slope, rainfall duration, particle median diameter, clay content of the soil, rill density and soil mass density.

(2) The sensitivity analysis reveals that the rainfall duration and the slope are important variables of the sediment transport process.

(3) An empirical model accepting the same input vector as the GRNN model is found successful with a general applicability.

(4) An empirical model that relates sediment load with rainfall intensity, slope and rainfall duration might be used for the gross approximation of the sediment load from bare no-rill surfaces, where information on particle size, density and clay content is not available. If one were to be provided with data of only slope, rainfall intensity and rainfall duration, a gross estimation of the total sediment load from bare land surfaces can be made in (kg/m²) by employing Eq. (7).

(5) The GRNN model can provide satisfactory estimates of the total sediment load from bare slopes, like the empirical models. However, due to the fact that the neural networks are not good extrapolators, the application of the GRNN model to another data set would require retraining and retesting.

(6) As opposed to the GRNN, the empirical model is not fully a black box. It reveals, at least conceptually, the physics of the process by relating the clay content, rill density, slope, rainfall intensity, rainfall duration, particle density and particle size to the total sediment load.

To submit a comment on this article please go to http://mc.manuscriptcentral.com/wej. For further information please see the Author Guidelines at wileyonlinelibrary.com

References

Abrahams, A.D., Li, G., Krishnan, C. and Atkinson, J.F. (1998) Predicting sediment transport by interrill overland flow on rough surfaces. *Earth Surface Processes and Landforms*, 23, 1087–1099.

Aksoy, H. and Kavvas, M.L. (2005) A review of hillslope and watershed scale erosion and sediment transport models. *Catena*, 64, 247–271.

Aksoy, H., Unal, N.E., Gedikli, A., Cokgor, S., Eris, E. and Yilmaz, M. (2011). Akarsu havzaları için yamaç ölçeğinde katı madde taşınım modeli geliştirilmesi. The Scientific and Technological Research Council of Turkey (TUBITAK) Report No. 108Y250, 194p. (in Turkish).

Aksoy, H., Unal, N.E., Cokgor, S., Gedikli, A., Yoon, J., Koca, K. *et al*. (2012) A rainfall simulator for laboratory-scale assessment of rainfall-runoff-sediment transport processes over a two-dimensional flume. *Catena*, 98, 63–72.

Aksoy, H., Unal, N.E., Cokgor, S., Gedikli, A., Yoon, J., Koca, K. *et al*. (2013) Laboratory experiments of sediment transport from bare soil with a rill. *Hydrological Sciences Journal*, 58(7), 1505–1518.

Aksoy, H., Gedikli, A., Erdem, N., Yilmaz, M., Eris, E., Yoon, J. *et al*. (2016) Rainfall-runoff model considering microtopography simulated in a laboratory erosion flume. *Water Resources Management*, 30(15), 5609–5624.

Aksoy, H., Eris, E. and Tayfur, G. (2017) Empirical sediment transport models based on indoor rainfall simulator and erosion flume experimental data. *Land Degradation & Development*, 28(4), 1320–1328.

Alp, M. and Cigizoğlu, H.K. (2007) Suspended sediment load estimation by two artificial neural network methods using hydrometeorological data. *Environmental Modelling & Software*, 22(1), 2–13.

Animka, S., Tirkey, P. and Nathawat, S. (2013) Use of satellite data, GIS and RUSLE for estimation of average annual soil loss in Daltonganj watershed of Jharkhand (India). *Journal of Remote Sensing Technology*, 1, 1.

Barfield, B.J., Barnhisel, R.I., Powell, J.L., Hirschi, M.C. and Moore, I.D. (1983) Erodibilities and eroded size distribution of Western Kentucky mine spoil and reconstructed topsoil. Institute for Mining and Minerals Research Final Report. Lexigton, KY: Univ. of Kentucky.

Cigizoglu, H.K. (2005). Generalized regression neural network in monthly flow forecasting. *Civil Engineering and Environmental Systems*, 22(2), 71–84.

Cigizoglu, H.K. and Alp, M. (2006) Generalized regression neural network in modelling river sediment yield. *Advances in Engineering Software*, 37(2), 63–68.

Desprats, J.F., Raclot, D., Rousseau, M., Cerdan, O., Garcin, M., Le Bissonnais, Y. *et al*. (2013) Mapping linear erosion features using high and very high resolution satellite imagery. *Land Degradation and Development*, 24, 22–32.

Fiorucci, F., Ardizzone, F., Rossi, M. and Torri, D. (2015) The use of stereoscopic satellite images to map rills and ephemeral gullies. *Remote Sensing*, 7, 14151–14178. Available at:doi:https://doi.org/10.3390/rs71014151.

Foster, G.R. (1982) Modeling the erosion process. In: Haan, C.T., Johnson, H.P. and Brakensiek, D.L. (Eds.) Hydrologic Modeling of Small Watersheds. Michigan: ASAE, St Joseph, pp. 295–380.

Ganasri, B.P. and Ramesh, H. (2016) Assessment of soil erosion by RUSLE model using remote sensing and GIS – a case study of Nethravathi basin. *Geoscience Frontiers*, 7, 953–961.

Gelagay, H.S. and Minale, M.S. (2016) Soil loss estimation using GIS and remote sensing techniques: a case of Koga watershed, Northwestern Ethiopia'. *International Soil and Water Conservation Research*, 4(2), 126–136.

Gilley, J.E., Kincaid, D.C., Elliot, W.J. and Laflen, J.M. (1992) Sediment delivery on rill and interrill areas. *Journal of Hydrology*, 140, 313–341.

Goldberg, D.E. (1989) Genetic Algorithms for Search, Optimization, and Machine Learning. Boston, MA, USA: Addison-Wesley.

Goldberg, D.E. (1999) Genetic Algorithms. USA: Addison-Wesley.

Govindaraju, R.S. and Kavvas, M.L. (1991) Modeling the erosion process over steep slopes- approximate analytical solutions. *Journal of Hydrology*, 127(1–4), 279–305.

Govindaraju, R.S. and Kavvas, M.L. (1992) Characterization of the rill geometry over strainght hillslopes through spatial scales. *Journal of Hydrology*, 130(1–4), 339–365.

Govindaraju, R.S., Kavvas, M.L., Tayfur, G. and Krone, R. (1992) Erosion control of decomposed granite at Buckhorn Summit. CALTRANS, Sacramento, California. Final Project Report.

Grismer, M.E. (2011) Rainfall simulation studies-a review of designs, performance and erosion measurement variability. California, USA: University of California-Davis. Research Report.

Guan, J. and Aral, M.M. (2005) Remediation system design with multiple uncertain parameters using fuzzy sets and genetic algorithm. *Journal of Hydrologic Engineering*, 10(5), 386–394.

Jain, A., Bhattacharjya, R.K. and Sanaga, S. (2004) Optimal design of composite channels using genetic algorithm. *Journal of Irrigation and Drainage Engineering*, 130(4), 286–295.

Julien, P.Y. (2010) Erosion and Sedimentation. Cambridge: Cambridge University Press.

Julien, P.Y. and Simons, D.B. (1985) Sediment transport capacity of overland flow. *Transactions of the ASAE*, 28(3), 755–762.

Katebikord, A., Darvishan, A.K. and Alavi, S.J. (2017) Changeability of erosion variables in small field plots from different rainfall durations with constant intensity. *Journal of African Earth Sciences*, 129, 751–758.

Kilinc, M. and Richardson, E.V. (1973) Mechanics of soil erosion from overland flow generated by simulated rainfall. Hydrology Papers, Fort Collins, Colorado: Colorado State University, Paper. 63.

Kim, S., Shiri, J., Kisi, O. and Singh, V.P. (2013) Estimating daily pan evaporation using different data-driven

methods and lag-time patterns. *Water Resources Management*, 27, 2267–2286.

de Lima, J.L.M.P., Dinis, P.A., Souza, C.S., de Lima, M.I.P., Cunha, P.P., Azevedo, J.M. et al. (2011) Patterns of grain-size temporal variation of sediment transported by overland flow associated with moving storms: interpreting soil flume experiments. *Natural Hazards and Earth System Science*, 11(9), 2605–2615.

Liong, S.Y., Chan, W.T. and Shreeram, J. (1995) Peak flow forecasting with genetic algorithm and SWMM. *Journal of Hydraulic Engineering*, 121(8), 613–617.

Merritt, W.S., Latcher, R.A. and Jakeman, A.J. (2003) A review of erosion and sediment transport models. *Environmental Modelling & Software*, 18, 761–799.

Meyer, L.D. and Wischmeier, W.H. (1969) Mathematical simulation of the process of soil erosion by water. *Transactions of the ASAE*, 12(6), 754–762.

Meyer, L.D., Foster, G.R. and Romkens, M.J.M. (1975) Source of soil eroded by water from upland slopes. In: Present and Prospective Technology for Predicting Sediment Yield and Sources, Proc. Sediment Yield Workshop, Oxford, MS, 28–30 November 1972. USDA-ARS-S-40, pp. 177–189.

Montenegro, A.A.A., Abrantes, J.R.C.B., de Lima, J.L.M.P., Singh, V.P. and Santos, T.E.M. (2013) Impact of mulching on soil and water dynamics under intermittent simulated rainfall. *Catena*, 109, 139–149.

Nord, G. and Esteves, M. (2005) PSEM_2D: a physically based model of erosion processes at the plot scale. *Water Resources Research*, 41, W08407.

Nunes, J.P., de Lima, J.L.M.P., Singh, V.P., de Lima, M.I.P. and Vieira, G.N. (2006) Numerical modeling of surface runoff and erosion due to moving rainstorms at the drainage basin scale. *Journal of Hydrology*, 330(3–4), 709–720.

Palisade Corporation. (2012) Evolver, The Genetic Algorithm Solver for Microsoft Excel 2012. New York, USA: Newfield.

Portner, N.B. and Schleiss, A.J. (2001) Discussion of modeling two-dimensional erosion process over infiltrating surfaces by Gokmen Tayfur. *Journal of Hydrologic Engineering*, 6(3), 259–262.

Romkens, M.J.M., Helming, K. and Prasad, S.N. (2002) Soil erosion under different rainfall intensities, surface roughness, and soil water regimes. *Catena*, 46, 103–123.

Seckin, N., Cobaner, M., Yurtal, R. and Haktanir, T. (2013) Comparison of artificial neural network methods with L-moments for estimating flood flow at ungauged sites: the case of East Mediterranean River basin, Turkey. *Water Resources Management*, 27, 2103–2124.

Sen, Z. and Oztopal, A. (2001) Genetic algorithms for the classification and prediction of precipitation occurrence. *Hydrological Sciences Journal*, 46(2), 255–267.

Sen, Z. (2004) Genetic Algorithm and Optimization Methods. Istanbul: Turkish Water Foundation Publications (in Turkish).

Shaker, A., Yan, W.Y. and Easa, S.M. (2010) Using stereo satellite imagery for topographic and transportation applications: an accuracy assessment. *GIScience and Remote Sensing*, 47, 321–337.

Singh, R.M. and Datta, B. (2006) Identification of groundwater pollution sources using GA-based linked simulation optimization model. *Journal of Hydrologic Engineering*, 11(2), 101–109.

Singer, M.J. and Walker, P.H. (1983) Rainfall—runoff in soil erosion with simulated rainfall, overland flow and cover. *Australian Journal of Soil Research*, 21, 109–122.

Storm, B., Jorgensen, G.H. and Styczen, M. (1987) Simulation of water flow and soil, erosion processes with a distributed physically-based modeling system. In: Forest Hydrology and Watershed Management. IAHS Publications, 167, 595–608.

Tayfur, G. (2001) Modelling two dimensional erosion process over infiltrating surfaces. *Journal of Hydrologic Engineering*, 6(3), 259–262.

Tayfur, G. (2002a) Applicability of sediment transport capacity models for nonsteady state erosion from steep slopes. *Journal of Hydrologic Engineering*, 7(3), 252–259.

Tayfur, G. (2002b) Artificial neural networks for sheet sediment transport. *Hydrological Sciences Journal*, 47(6), 879–892.

Tayfur, G. (2009) GA-optimized method predicts dispersion coefficient in natural channels. *Hydrology Research*, 40(1), 65–78.

Tayfur, G. (2012) Soft Computing in Water Resources Engineering. Southampton, United Kingdom: WIT Press.

Tayfur, G. (2017) Modern optimization methods in water resources planning, engineering and management. *Water Resources Management*, 31(10), 3205–3233.

Tayfur, G. and Singh, V.P. (2004) Numerical model for sediment transport over nonplanar, nonhomogeneous surfaces. *Journal of Hydrologic Engineering*, 9(1), 35–41.

Tayfur, G., Moramarco, T. and Singh, V.P. (2007) Predicting and forecasting flow discharge at sites receiving significant lateral inflow. *Hydrological Processes*, 21, 1848–1859.

Tayfur, G. and Moramarco, T. (2008) Predicting hourly-based flow discharge hydrographs from level data using genetic algorithms. *Journal of Hydrology*, 352(1–2), 77–93.

Tayfur, G., Barbetta, S. and Moramarco, T. (2009) Genetic algorithm-based discharge estimation at sites receiving lateral inflows. *Journal of Hydrologic Engineering*, 14(5), 463–474.

Tayfur, G. and Singh, V.P. (2011) Predicting mean and bankfull discharge from channel cross-sectional area by expert and regression methods. *Water Resources Management*, 25(5), 1253–1267.

Tsoukalas, L.H. and Uhrig, R.E. (1997) Fuzzy and Neural Approaches in Engineering. New York, NY, USA: Wiley.

Wischmeier, W.H., Johnson, C.B. and Cross, B.V. (1971) A soil erodibility monograph for farmland and construction sites. *Journal of Soil and Water Conservation*, 26(5), 189–193.

Yuksel, A., Gundogan, R. and Akay, A.E. (2008) Using the remote sensing and GIS technology for erosion risk mapping of Kartalkaya Dam Watershed in Kahramanmaras, Turkey. *Sensors (Basel)*, 8(8), 4851–4865.

Zhang, G.H., Liu, Y.M., Han, Y.F. and Zhang, X.C. (2009) Sediment transport and soil detachment on steep slopes: I. Transport capacity estimation. *Soil Science Society of America Journal*, 73(4), 1291–1297.